Mapping Forest Regeneration from Terrestrial Laser Scans

Gábor BROLLY[*] – Géza KIRÁLY – Kornél CZIMBER

Department of Forest Opening Up, Institute of Geomatics and Civil Engineering,
Faculty of Forestry, University of West Hungary, Sopron, Hungary

Abstract – Location, spread, abundance and density of forest regeneration are key factors in understanding forest dynamics as well as in operational management of uneven-aged stands. Simulation of forest growth, silviculture and planning of skid road networks require accurate and objective methods for locating forest regeneration. Terrestrial laser scanning has high potential for tree mapping, however, the development of automatic processing methods has been focused on mature trees so far. This study introduces an automatic procedure to locate individual trees with 3–6 meter height from terrestrial laser scanner data. The method has been validated on three sample quadrates representing different stand structures and it succeeded in detecting 79–90% of trees extracted manually from the point cloud. Out of the investigated stand features, stem density had the strongest impact on the performance, while branching intensity slightly affected the detection rate. The results highlight that terrestrial laser scanning has the ability for the quantitative evaluation of regeneration, providing a prospective tool for surveying forests of contiguous cover.

LIDAR / TLS / forestry / tree detection / regeneration / voxel

Kivonat – Erdei újulat térképezése földi lézeres letapogatás adataiból. Az erdei újulati foltok helye, kiterjedése, borítottsága és törzsszáma kulcsfontosságú tényezők az erdődinamikai folyamatok feltárásában és a többkorú faállományok kezelésében. A fatermési modellek előállítása, az üzemi gyakorlatban végzett erdőművelés valamint erdőfeltárás pontos és objektív módszereket kíván az újulat helyének meghatározására. A földi lézeres letapogatás kiválóan alkalmas törzstérképek előállítására, ám az adatok feldolgozásához szükséges eljárásokat eddig csak szálerdőkre fejlesztettek ki. A tanulmány olyan automatikus eljárást mutat be, ami 3–6 méter magasságú faegyedek lézeres letapogatás adataiból történő azonosítását teszi lehetővé. Három, különböző jellegű újulati foltban létesített mintaterületen a ponthalmaz vizuális interpretációjával azonosított törzsek 79–90%-át sikerült automatikus úton felismerni. Az eljárás teljesítményét a vizsgált állományjellemzők közül elsősorban a törzsszám befolyásolta, míg az ágak mennyiségének hatása elenyésző. Az elért eredmények rámutatnak, hogy a földi lézeres letapogatás alkalmas az újulat mennyiségének felmérésére, így a folyamatos borítású erdők leírásának ígéretes eszköze lehet.

LIDAR / földi lézerszkennelés / erdészet / újulat / faegyed kimutatása / voxel

---

[*] Gábor Brolly: gbrolly@emk.nyme.hu; H-9400 SOPRON, Bajcsy-Zs. u. 4.

1   INTRODUCTION

The expansion of nature-based silviculture in Europe has been generating variability in age and complexity in structure of forest stands. In forests of contiguous cover, the development of the regeneration strongly depends on the adjacent mature trees through the allocation of light and nutrients. Operational planning, treatment and administrative control of uneven-aged stands require detailed geospatial information on trees with heterogeneous size. For instance, the location of both mature trees and regeneration patches must be taken into consideration at marking trees for cutting or at decision support in forest opening up e.g. planning the fine network of transportation paths.

Moreover, a geospatial database including mature trees and regeneration has apparent value as input for scientific purposes to understand forest growth or to simulate the effects of regeneration cuttings. To locate trees of heterogeneous size, a sensor is needed with (1) effective range to record objects at a distance of at least 30 meter and (2) capacity of identifying fine structures such as juvenile tree stems.

Terrestrial laser scanning (TLS) is an active remote sensing technology holding great promise for supporting forestry applications. TLS data capture results in 3D point cloud of object surfaces that can be processed by visual interpretation (Hopkinson et al. 2004, Watt – Donoghue 2005) or automatic procedures (Aschoff – Spiecker 2004, Bienert et al. 2007). The output involves the map of individual stem locations and the related tree metrics; typically diameter at breast height (DBH) and tree height. The location and estimation accuracies of the derived tree models are in accordance with the requirements of operational forestry, which has been confirmed in studies of various geographic regions over the temperate zone (e.g. Király – Brolly 2007). It is not surprising that most of the investigations concluded that TLS has high potential in supporting ground-based forest inventories (Thies – Spiecker 2004, Pueschel et al. 2013). Moreover, TLS-derived tree attributes can be combined with airborne laser scans to extend the parameter retrieval into larger area (Lindberg et al. 2012).

Algorithms on tree detection and DBH estimation imply that stems can be approximated by a cylinder in a given height interval, therefore their horizontal cross-section has circular shape (Simonse et al. 2003). Usefulness of this assumption on stem geometry has been verified in two and three-dimensional stem mapping approaches (Brolly – Király 2009a). In comparison to mature trees, juvenile ones intercept fewer point measurements at a constant distance from the scanner because they cover smaller area. In addition, point measurements are frequently scattered on the rough surface of stems. Since the amount of stem surface points is low and their pattern introduces high degree of irregularity, the existing tree mapping methods have difficulties in detecting juvenile trees. However, the high sampling density of TLS allows for the automatic detection of thin linear features such as twigs suggesting the possibility to detect juvenile trees from the point cloud. For instance, Bucksch and Fleck (2011) scanned trees from four directions at a distance of about four meters with angular step width of 0.036 degrees. The automatic extraction of branch structure resulted correlation of up to 0.99 in comparison to manually measured branch diameters.

The amount and spatial distribution of light transmitted through the upper canopy specify the density, composition and growth of the regeneration, therefore crown models are essential for the investigation of the eco-physiological process of trees and the simulation of gap dynamics. In addition to tree positions, 3D structural models including stem and crown can be derived from the point cloud. Crown models account for the originating and end point of the branches as well as their length, diameter and orientation. Branches have been modelled as a set of cylinders in telescopic arrangement whose parameters were specified by minimizing the squared distance of the surface and the corresponding point measurements (Pfeifer et al. 2004). Gorte and Pfeifer (2004) proposed a directed graph structure to reveal branch hierarchy

by storing the preceding and succeeding shoots in each node. Bucksch and Fleck (2011) demonstrated the capacity of high-density TLS data to reconstruct the fine structure of tree crowns including twigs with diameter of 1–2 cm. Danson et al. (2007) developed a procedure for the assessment of directional canopy gap fraction, which showed good agreement with the estimates derived from hemispherical photos. Henning and Radtke (2006) estimated Plant Area Index (PAI) by converting the TLS point cloud in a 3D grid structure and assessing the presence of vegetable matter upon the number of pulses passing through each cell and the number of intercepted pulses. Coté et al. (2009) created architectural model of trees from TLS data to provide basis for the computation of reflectance properties of the canopy in a radiation transfer analysis.

Although TLS has been used extensively to investigate the upper canopy, there has been little effort to take advantage of this technique in studying the structure of understory. Characteristics of the stand structure at the age of 'saplings' (achieving 3–6 meter height) are similarly important from ecologic respect as trees tend to vary in height, form and quality at this age thus the competition is especially strong. Mapping and structural reconstruction of juvenile trees based on in-situ TLS data has been still challenging, as present tree detection methods are not suitable for the recognition of small vegetation components in the understory.

This study is focusing on the development of automatic detection of trees with height of 3–6 m from the point cloud to extend the use of TLS over stands of contiguous forest cover and in this way, widen its field of potential applications in forestry. The method presented in this paper has been introduced in a PhD thesis (Brolly 2013).

2 MATERIAL AND METHOD

Juvenile tree mapping has to meet some specific requirements. First, 3D approaches are preferred because the horizontal slices of the point cloud provide few stem surface points for reliable detection. In regrowth patches, considerable amount of data is returned from irrelevant entities, such as branches and foliage surrounding the stems, which must be eliminated by filtering. Filtering of irrelevant data can be regarded as a classification according to 'stem' or 'other vegetation components'. Natural forest regeneration is characterized by high density and heavy branching resulting in data gaps in stem point measurements or even occlusion of trees especially farther from the scanner. Stem detection algorithm must overcome data discontinuity by the aggregation of the corresponding tree fragments.

Considering these expectations, the developed procedure is composed of two modules, i.e. filtering and objects detection addressing the following issues:

1. Conversion of the point cloud into regular 3D data structure
2. Filtering of irrelevant data, including side branches and leaves
3. Reconstruction of stems by the aggregation of stem fragments.

2.1 Sample site

The algorithm was validated on a terrestrial laser scanner point cloud captured in the region of Pilisszentkereszt (N47.722, E18.860), Hungary, in the altitude of 430–500 meters. The multi-layered stand is composed of 55% beech (*Fagus sylvatica*), 23% sessile oak (*Quercus petraea*) and 12% hornbeam (*Carpinus betulus*) over 10.5 ha area. The mean age of trees associated with the dominant and subdominant canopy layers was 100 and 50 years respectively at the data acquisition. The site has been subject to long-term regeneration managed by the Pilisi Parkerdő Zrt according to the Pro Silva directives since 1999, which resulted in 2–10 meter high natural regeneration patches.

Three quadrates of 5×5 meters labelled with 'P1', 'P2' and 'P3' were delineated within three distinct regeneration patches. All the sample quadrates are located in a slope of 10° with South-West aspect and characterized by different stem density and branching frequency. Both factors are expected to have influence on tree detection because stem density is related to the degree of occlusion while branches generate irrelevant point measurements being potential error sources.

Stem positions were identified by visual interpretation of the point cloud and they were used as reference trees for the assessment of the automatic stem detection. Stem positions were located at 1.30 meter height above ground level following the manual filtering of stem point measurements. Only the trees with height exceeding two meters were involved in the reference data set. Branching frequency was assessed subjectively for each quadrate during the interpretation. Sample quadrate P1 is considered as the simplest case as stem counts ($n_1 = 41$ trees) and branching frequency are relatively low here. The quadrate P2 is characterized by the highest stem density ($n_2 = 212$). Trees ($n_3 = 58$) within quadrate P3 have wider crown relative to the trees within the two other quadrates. The shrub-layer is of 0.5 meter height with low abundance; therefore, it has little influence on the stem detection.

2.2 Data acquisition

The whole study site was scanned in leaf-less state of the stand by combining the data captured from 38 scanning positions using Riegl LMS-Z 420i instrument on April 2009. The range finding unit of the instrument utilizes near infrared laser with beam divergence of 0.25 mrad (Riegl, 2010). The scanning was conducted at tilted axis of +50° and –30° applying angular stepwidth of 0.07° for horizontal and vertical direction. The point cloud was recorded and georeferenced by the piLine Ltd. The mean 3D error of the georeferencing was 0.05 meter. The digital terrain model (DTM) of the study site as well as the map of mature trees (DBH>10 cm) were created in the course of previous studies (Brolly – Király 2009b). The location of the three sample quadrates and the arrangement of scanning positions are depicted in *Figure 1*.
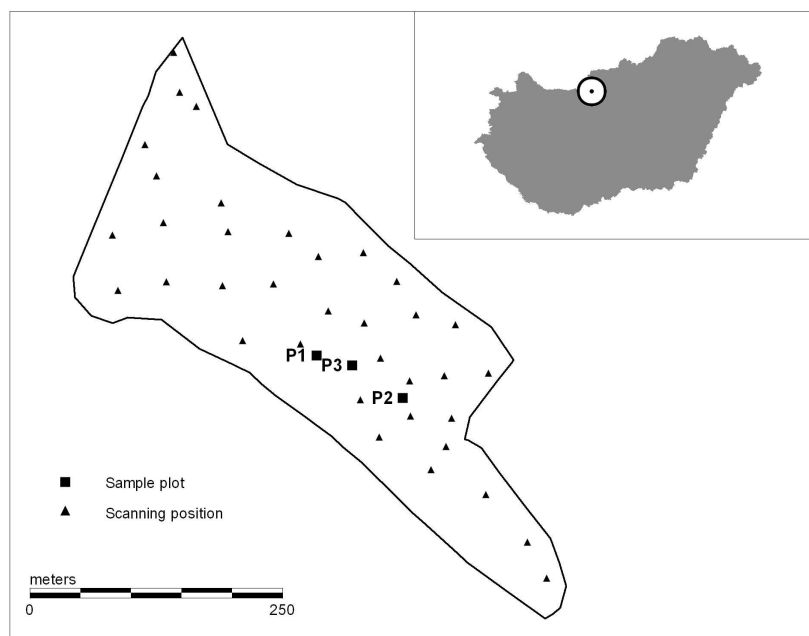
Figure 1. Sample quadrates and scanning positions on the study site

2.3 Data structure

Tree models created in this study are composed of connected cubic elements of equal size also referred to as volumetric elements or briefly *voxels* (Kaufman et al. 1993). The associated voxel space is a kind of grid data structure that can be considered as the extension of raster data structure into the 3D domain. Owing to the regular construction, neighbourhood relations are relatively simple to characterize; a single voxel can share six faces, twelve sides and eight vertices with maximum 26 connected neighbours. Voxel data structure can be used effectively in object detection by adapting the tools of digital image processing so it has appeared optimal for the extraction of juvenile trees.

The georeferenced point cloud was converted into a binary voxel space. Voxels containing at least one point measurements were set to 'filled'. The vertical extent of the voxel space was limited to the elevation between 0.5 and 3.5 meters above the DTM as this interval is dominated by stem surface points.

The grid resolution was specified by visual evaluation of voxel space subsets with different voxel size. Voxel size of 5 cm deemed adequate for all the sample quadrates considering point spacing within the quadrates and the size of trees to be detected.

Adjacent filled voxels constitute connected regions. The smallest region consists of a single voxel, i.e. each voxel belongs to exactly one connected region. Connected regions can be delineated using region growing algorithms, e.g. the Connected Component Labelling (Jain et al. 1995). Connected voxel regions can be translated to *voxel objects* by creating a spatial database that allows identification and access of the unique regions. Voxel objects can be characterized by attributes concerning their geometry and neighbourhood relations. Juvenile trees are usually represented by multiple voxel objects due to the obscuring effects of neighbouring stems and the resulting data gaps. In order to assess the stem number and locate individual tree positions, the corresponding voxel objects must be aggregated. The set of coherent voxel objects can be regarded as one *disconnected voxel object*, representing a complete tree model composed of isolated tree fragments.

2.4 Filtering

Juvenile tree stems can be visually perceived as linear patterns surrounded by irregularly distributed data with altering density originating from branches and dry leaves. In juvenile age, stems and crowns are not separated into distinct vertical zones because the natural pruning has just begun. The crown and lateral branches of juvenile trees generate considerable amount of laser returns. These data are irrelevant for tree mapping; furthermore, they induce false detections. To reduce irrelevant data, a local filtering was developed.

The structuring element used in the filtering defines a 3D region of space around its central voxel. The filtering value is defined as the counts of filled voxels within the defined region. The shape of the structuring element must ensure high filtering values for vertically elongated features. To design appropriate structural element, the following guidelines should be taken into account: (1) The filtering is anisotropic in vertical direction hence the structuring element must be elongated along its vertical axis. (2) The filtering has no preference in horizontal direction so the structuring element is radially symmetric. (3) The filtering must be tolerant of vertical direction because of leaning stems thus the size of the structuring element widens out around the central voxel. These considerations lead to the structure illustrated in *Figure 2*.

The filtering value is computed for each filled voxel. Voxels with filtering value below a predefined threshold are assumed to be vegetation components apart from stems so they can be removed from the data set. The parameters of the filtering applied in this study were the following: radius = 5, height = 11, threshold of filtering value $\geq$ 5. (Dimensions refer to spacing between voxel midpoints.)
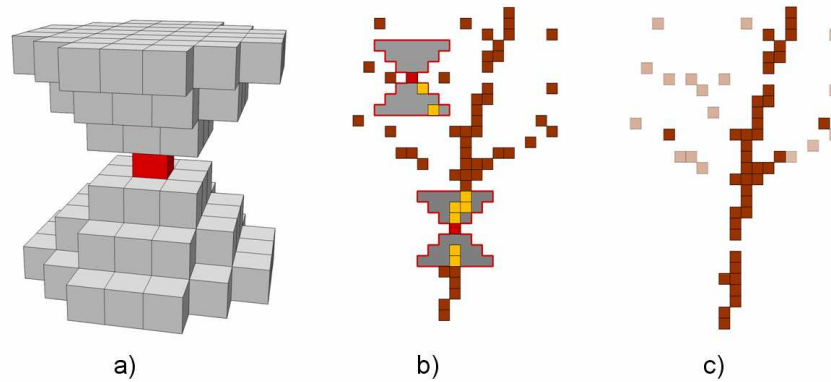
Figure 2. Filtering of irrelevant data. a) Structuring element with radius of three voxels and height of six voxels, (b-c) the concept of the operation

2.5 Reconstruction of stems from fragments

Adjacent voxels in any of the 26 directions are organized into objects by Connected Component Labelling algorithm. Stems are usually composed of multiple objects due to data discontinuity resulting from the obscuring effects of neighbouring trees. Voxel objects representing stem fragments are the basic elements of the subsequent reconstruction procedure. It is practical to generalize the objects to one-voxel-thin *vertical axis* representing the horizontal dimension and orientation of the fragments. *Vertical axis* of a contiguous object is defined as the set of connected voxels with solely upper or lower adjacency (lateral adjacency is forbidden). In this way, the voxel count of a vertical axis is the same as the vertical extent of the object. However, since diagonal adjacency is also allowed, its shape is not necessarily vertical. Vertical axes are extracted by finding the shortest path between the lowest and the highest voxel of the objects. To do so, objects are represented as graphs where the vertices correspond to voxel positions and the edges denote adjacency relations. The shortest path within the resulting graph is obtained by using Dijkstra's algorithm (Cormen et al. 1990). Objects in which no path without lateral adjacency between the highest and lowest voxel exists, are considered atypical for representing young trees. In this case, the region remains in the voxel space but it is excluded from the subsequent processing so it cannot be used in stem reconstruction.

Voxel objects (i.e. vertical axes) represent fragments of either stems or branches; however, they cannot be distinguished based on their shape properties. In the next step, objects that belong to each other are aggregated into disconnected voxel objects representing complete trees. High number of combinations among the objects is possible, so a rule set is needed which favours to the aggregation of stem fragments and skip the branches. Three assumptions have been formulated concerning the shape of stems. (1) Stems are vertically extensive features. (2) The shape of stems is approximately straight. (3) Overlying fragments are vertically close to each other; data gaps separating them are short.

Considering these theories, three variables have been introduced to reveal the spatial relationship of any two fragments within the voxel space. Knowing the coordinates of the voxels constituting the vertical axes, the Euclidian distance between the end voxels as well as the path length between them is computed as input. The three variables stand for the extent (E), shape (S) and gap distance (G) of the resulting disconnected vertical axis. Detailed derivation of the formulae can be found in Brolly (2013). Each of the variables is normalized into the interval of [0, 1] with the theoretically maximum return value of the corresponding function. The degree of conformity of the disconnected vertical axis to the hypothetical stem shape is quantified using the aggregation factor A, which is yielded as the product of the three variables:

$$A = E \cdot S \cdot G$$

Computation of A can be extended over the aggregation of disconnected vertical axes so a stem can consist of any number of fragments.

    The algorithm initiates by the computation of A for any possible object pairs. The aggregation takes place in the order of descending value of A, so the assignment resulting in highest degree of conformity to the assumed stem shape is realized first (*Figure 3*). Following each aggregation, the values of A with respect to its neighbouring objects are recomputed. As vertical axes contain only vertical or diagonal adjacency, the size of any object (regardless its continuity) is limited to the vertical extent of the voxel space. The aggregation routine is being iterated until the threshold of 0.01 on the aggregation value of potential object pairs is exceeded. This threshold prevents the aggregation of distant fragments that probably belong to different trees. The majority of the resulting disconnected objects represent stem fragments although some of them constitute branches or meaningless groups of voxels arranged accidentally in linear pattern. Tree stems are assumed to be the largest vertical features within regrowth patches, so voxel counts of disconnected objects can be used to distinguish stems from other vegetation fragments. The optimal threshold of 20 voxels was specified by visual evaluation of the classification in the three sample quadrates. Lower thresholds resulted in misclassified branches, while higher ones lead to omission of stems.
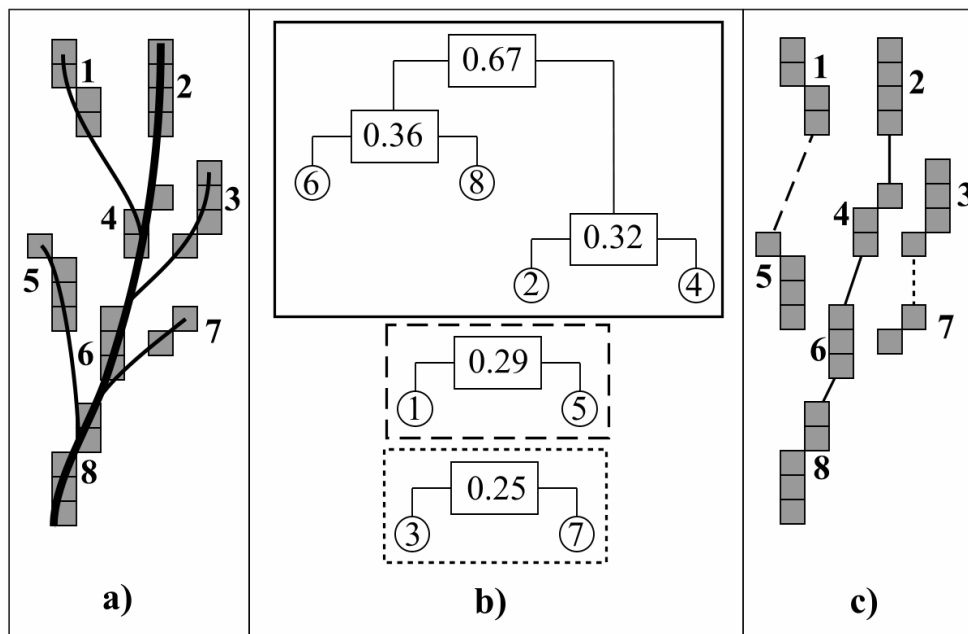

Figure 3. Aggregation of tree fragments. a) Components represented as voxel objects labelled by 1–8, b) Assignment according to the maximum of aggregation factor, c) Resulting disconnected objects composed of fragments (1, 5); (2, 4, 6, 8) and (3, 7)

3   RESULTS AND DISCUSSION
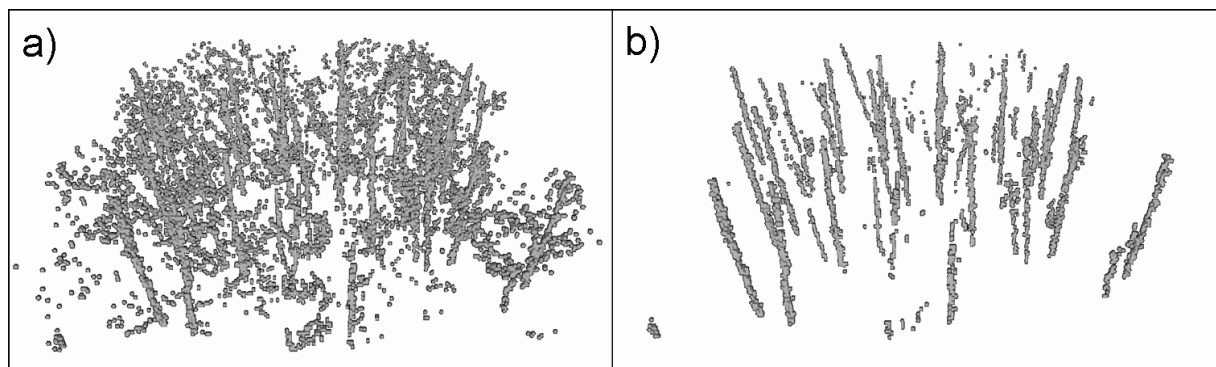
3.1 Filtering

Filtering is considered efficient if surface points of irrelevant vegetation are reduced but stem point measurements are preserved. The proportion of eliminated points indicates filtering intensity, while the retained stem surface points denote filtering reliability. Filtering is a pre-processing step of tree mapping, so its actual value emerges indirectly in the results of stem detection.

The performance of anisotropic filtering in sample quadrates P1, P2 and P3 is given in *Table 1*. The majority of the total voxels has been eliminated from quadrates P1 and P3. The relative low filtering intensity in quadrate P2 is explained with high stem density resulting in elevated number of stem voxels. Although at P3, where the stem density is 34% higher relative to that of P1, the filtering intensity is only slightly different. Higher voxel counts per individuals in P3 indicate larger crown size and / or higher degree of branching frequency, which has been only partially removed by the filtering.

The proposed anisotropic filtering is adequate to remove irrelevant data arranged in random pattern *(Figure 4)* preserving stems even if their main orientation is inclined. According to this tolerance in orientation, acute-angled branches cannot be removed by this filtering method.

Table 1. The effect of the filtering on data amount within the sample quadrates

Quadrate	Tree counts	Voxel counts		Voxel counts / tree	
		Original	Removed [%]	Original	Preserved
P1	41	11806	58.0	228	121
P2	212	38371	36.8	181	114
P3	58	22020	58.8	380	156

Figure 4. a) Perspective view of the voxel space generated from the total measurement data of sample quadrate P1. b) The result of filtering

3.2 Tree mapping

The tree detection algorithm provides tree positions in a given reference height and the vertical axis of stems. Knowing tree positions, the boundary of regrowth patches can be delineated and stem density within the patches can be estimated directly.

The validation of extracted tree positions for the sample quadrates are given in *Table 2*. Correct detections refer to extracted stem positions with matching reference trees within a positional tolerance of 10 cm. The matching must be unambiguous, i.e. exactly one reference tree can be assigned to a given model position and vice versa. Omissions are undetected trees, while misclassifications are false detections. Omission rate is normalized by the total number of reference trees, thus it complements detection rate to 100%. Misclassification rate is proportional to the number of correct detections.

The highest detection rate was achieved in quadrate P1, where both stem density and branching frequency are moderate. The highest omission rate as well as the highest misclassification rate was found in quadrate P2 where the stem density is the highest. Stem density appears to have the main impact on the overall performance of stem detection.

Although stem density in P2 is over three times greater than in the other two quadrates, the corresponding reduction in detection rate is relative low. Due to the high branching frequency in P3, the filtering was less effective so the remaining tree fragments show high diversity in shape. Detection rate of 87.9% only slightly underperforms that of achieved in quadrate P1 (90.2%), implying that branching frequency has minor relevance on stem detection. This can be traced back to the generalization of voxel regions to vertical axes, as the latter represent the branch-free subset of stem fragments. Generalization of objects to their vertical axis can be regarded as a kind of filtering as well that highlights the main direction of the objects and eliminates the remaining parts irrespective of the degree of structural complexity.

Table 2. Results of the automatic tree detection

Sample quadrate	P1	P2	P3
Reference trees	41	212	58
Correct [%]	90.2	79.3	87.9
Omission [%]	9.8	20.7	12.1
Misclassification [%]	9.8	25.7	10.5

3.3 Modelling

The reconstructed stems are illustrated in *Figure 5*. The individuals are represented in the voxel space by their generalized vertical axes. Due to data discontinuity, the vertical axes are composed fragments resulting in disconnected models. This concept enables to reconstruct standing juvenile trees including the slightly inclined ones.

Tree models at the three sample quadrates differ in structural properties, which are attributed to the distinct stand characteristics *(Table 3)*. Although tree density is considerably different in sample quadrates P1 and P2, the fragmentation degree (i.e. the number of objects having been connected for each detected stem) is almost the same. Undetected stems in P2 are assumed to be fragmented more so that the resulting aggregated objects are too small and they cannot be classified as stems.

Detection rate shows close agreement with mean voxel counts composing the vertical axes. There is no difference in height among the tree models because the vertical extent of the voxel spaces is limited to the stem region, which is equal for the three sample areas. So the reason for the variation in voxel counts of vertical axes is not the diversity in height but the ratio in size of fragments and data gaps. High stem density in P2 is assumed to result smaller fragments separated by larger data gaps. Vertical axes composed of fewer voxels explains the higher omission rate.

One could expect that the heavy branching in P3 generate higher degree of occlusion consequently higher degree of fragmentation. As the mean object counts is the lowest in this quadrate, it seems the leaf-less lateral branches are too thin to cause data discontinuity at the applied voxel resolution thus branching had small impact on stem detection.

Table 3. Fragmentation degree of tree models

Sample quadrate	P1	P2	P3
Mean object counts / tree	3.8	3.8	2.9
Maximum object counts / tree	9	9	8
Mean voxel counts (vertical axis) / tree	45.4	38.8	47.7
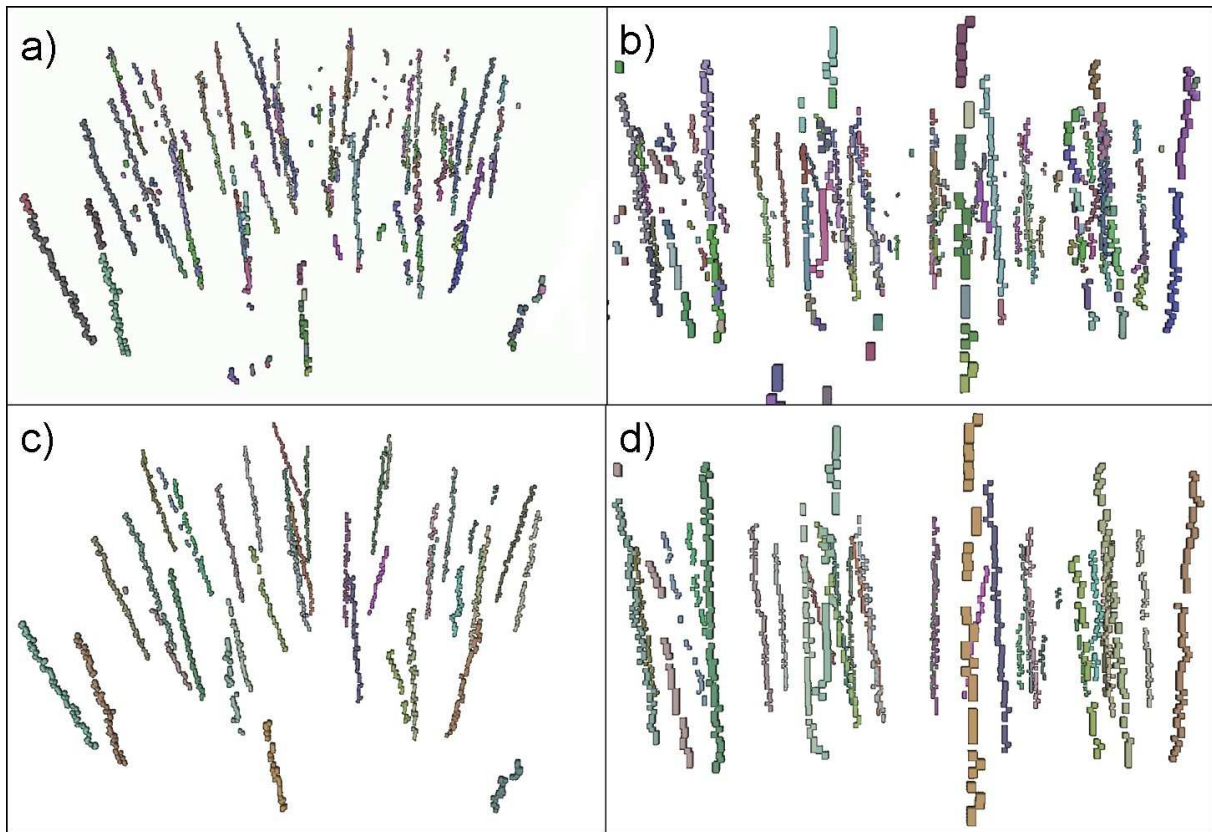
Figure 5. Reconstruction of juvenile tree stems. Fragments are distinct objects without thematic coherence indicated by different colours. a) Perspective view of the fragments over the sample quadrate P1, b) front view of a magnified subset. Following the aggregation, the corresponding fragments constitute stem models represented by identical colours. c) Perspective view of the disconnected stem models in sample quadrate P1, d) front view of a magnified subset

The overall performance of tree mapping and modelling depends on the method used for the calculation of shape properties and on the rule of object aggregation. The advantage of the presented stem detecting algorithm is that only two parameters (threshold on the aggregation factor and threshold on the voxel counts) are needed to control the aggregation of stem fragments and to classify disconnected voxel objects. It is assumed that the optimal value of these two parameters can be found iteratively by refinement either of the parameters and checking the result. A prospective way for developing the aggregation rule has been suggested where each object is represented by a cylinder along its axis and the pair-wise overlaps between the cylinders are checked. It is assumed that the using of overlapping cylinders would especially be powerful if they were representing the variation in diameter, as two stem fragments are more likely to be coherent if their diameter is similar. Since the algorithm does not take diameter in account at present stage, this is a potential way of development. However, measuring diameters of juvenile trees requires voxel size of approximately one centimetre, which is five-times smaller than what was used in this study.

4 CONCLUSION

The proposed algorithm allows for mapping of juvenile trees in regeneration patches with comparable detection rate achieved by recent automatic methods applied at mapping of mature trees. This highlights the potential of high-resolution TLS data to characterise understory vegetation.

To detect juvenile trees with fine structure, three-dimensional data structure is suggested. In contrast, there is a wide range of methods for mapping mature trees by various, computationally less demanding two-dimensional approaches. Detection of juvenile stems requires considerably high data density. Spacing of laser point measurements successively decreases afar from the scanner, putting limitation to the effective detection range surrounding a single scanning position. For operational mapping of uneven aged stands by TLS, a multi-level approach seems to be practical, where mature trees are extracted by using two-dimensional methods followed by the detection of juvenile trees within regeneration patches. Regeneration patches could be delineated using interpretation of the density map of the TLS point cloud within the height interval of 1–4 meters above the DTM. Limitation in mapping range from a single scanning has economic issue at practical surveying of large areas through the increased number of station set-ups; therefore, the proposed method is advisable rather for plot-based sampling of regeneration. Despite the effective filtering of point measurements being relevant for tree mapping purpose, the extraction of seedlings smaller than a few meters is still challenging because of their similarity in structure to shrubs and herbal vegetation. The proposed algorithm was designed to detect and reconstruct broadleaved stems in leaf-less state. Leaf-less state is highly recommended for scanning regeneration to minimize obscuring effects from leaves, however, it hinder the classification of tree species even using full-waveform information. As the geometric properties of conifers considerably different, the mapping of conifer regeneration needs further investigations.

REFERENCES

ASCHOFF, T. – SPIECKER, H. (2004): Algorithms for the automatic detection of trees in laser scanner data. In: Proceedings of the ISPRS working group VIII/2, "Laser-Scanners for forest and Landscape assessment". Freiburg, Germany. 3-6 October 2004. 71-75.

BIENERT, A. – SCHELLER, S. – KEANE, E. – MOHAN, F. – NUGENT, C. (2007): Tree detection and diameter estimations by analysis of forest terrestrial laserscanner point clouds. International Archives of Photogrammetry, Remote Sensing and Spatial Information Sciences 36 (3/W52), 50–55.

BROLLY, G. – KIRÁLY, G. (2009a): Algorithms for stem mapping by means of Terrestrial Laser Scanning. Acta Silvatica et Lignaria Hungarica 5: 119–130.

BROLLY, G. – KIRÁLY, G. (2009b): Lézeres letapogatás feldolgozása erdei környezetben. [Processing laser scans over forested environment.] In: Lakatos, F. – Kui, B. (eds.): Nyugat-magyarországi Egyetem, Erdőmérnöki Kar: Kari Tudományos Konferencia Kiadvány. Sopron. 12 October 2009. 29–34. (in Hungarian)

BROLLY, G. (2013): Locating and parameter retrieval of individual trees from terrestrial laser scanner data. Ph.D. dissertation, University of West Hungary, Sopron, Hungary, 104 p. Online: http://ilex.efe.hu/PhD/emk/brollygabor/disszertacio.pdf

BUCKSCH, A. – FLECK, S. (2011): Automated detection of branch dimensions in woody skeletons of fruit tree canopies. Photogrammetric Engineering and Remote Sensing 77 (3): 229–240.

CORMEN, T. H. – LEISERSON, C.F. – RIVEST, R.L. (1990): Algoritmusok. [Algorithms] Műszaki Könyvkiadó, Budapest. 884 p. (in Hungarian)

COTE, J.F. – WIDLOWSKI, J.L. – FOURNIER, R.A. – VERSTRAETE, M.M. (2009): The structural and radiative consistency of three-dimensional tree reconstructions from terrestrial lidar. Remote Sensing of Environment 113: 1067–1081.

DANSON, F.M. – HETHERINGTON, D. – MORSDORF, F. – KOETZ, B. – ALLGÖWER, B. (2007): Forest Canopy Gap Fraction From Terrestrial Laser Scanning. IEEE Geoscience and remote sensing letters 4 (1): 157–161.

GORTE, B. – PFEIFER, N. (2004): Structuring laser-scanned trees using 3d mathematical morphology. ISPRS- International Archives of Photogrammetry, Remote Sensing and Spatial Information Sciences 35 (Part B): 39–45.

HENNING, J.G. – RADTKE, P.J. (2006): Ground-based laser imaging for assessing three-dimensional forest canopy structure. Photogrammetric Engineering and Remote Sensing 72 (12): 1349–1358.

HOPKINSON, C. – CHASMER, L. – YOUNG-POW, C. – TREITZ, P. (2004): Assessing forest metrics with a ground-based scanning LIDAR. Canadian Journal of Forest Research. 34: 573–583.

JAIN, R. – KASTURI, R. – SCHUNCK, B.G. (1995): Machine Vision. McGraw-Hill, Inc., ISBN 0-07-032018-7; 549 p.

KAUFMAN, A. – COHEN, D. – YAGEL, R. (1993): Volume graphics. IEEE Computer 26 (7): 51–64.

KIRÁLY, G. – BROLLY, G. (2007): Tree height estimation methods for terrestrial laser scanning in a forest reserve. International Archives of Photogrammetry, Remote Sensing and Spatial Information Sciences. 36 (3/W52): 211–215.

LINDBERG, E. – HOLMGREN, J. – OLOFSSON, K. – OLSSON, H. (2012): Estimation of stem attributes using a combination of terrestrial and airborne laser scanning. European Journal of Forest Research 131 (6): 1917–1931.

PFEIFER, N. – GORTE, B. – WINTERHALDER, D. (2004): Automatic reconstruction of single trees from terrestrial laser scanner data. ISPRS- International Archives of Photogrammetry, Remote Sensing and Spatial Information Sciences 35 (Part B): 114–119.

PRO SILVA (2012): Pro Silva Principles. Pro Silva Europe. 69 p. Online: www.prosilvaeurope.org

PUESCHEL, P. – NEWNHAM, G. – ROCK, G. – UDELHOVEN, T. – WERNER W. – HILL, J. (2013): The influence of scan mode and circle fitting on tree stem detection, stem diameter and volume extraction from terrestrial laser scans. ISPRS Journal of Photogrammetry and Remote Sensing 77 (1): 44–56.

RIEGL (2010): Data sheet LMS-Z420i, 03/05/2010. Riegl Laser Measurement System GmbH, Horn, Austria. Online: www.riegl.com

SIMONSE, M. – ASCHOFF, T. – SPIECKER, H. – THIES, M. (2003): Automatic determination of forest inventory parameters using terrestrial laser scanning. In: Proceedings of the ScandLaser Scientific Workshop on Airborne Laser Scanning of Forests. Umea, Sweden. 2–4 September, 2003. 271–257.

THIES, M. – SPIECKER, H. (2004): Evaluation and future prospects of terrestrial laser scanning for standardized forest inventories. In: Proceedings of the ISPRS working group VIII/2, "Laser-Scanners for forest and Landscape assessment". Freiburg, Germany. 3–6 October 2004. 192–198.

WATT, P.J. – DONOGHUE, D.N.M. (2005): Measuring forest structure with terrestrial laser scanning. International Journal of Remote Sensing 26 (7): 1437–1446.